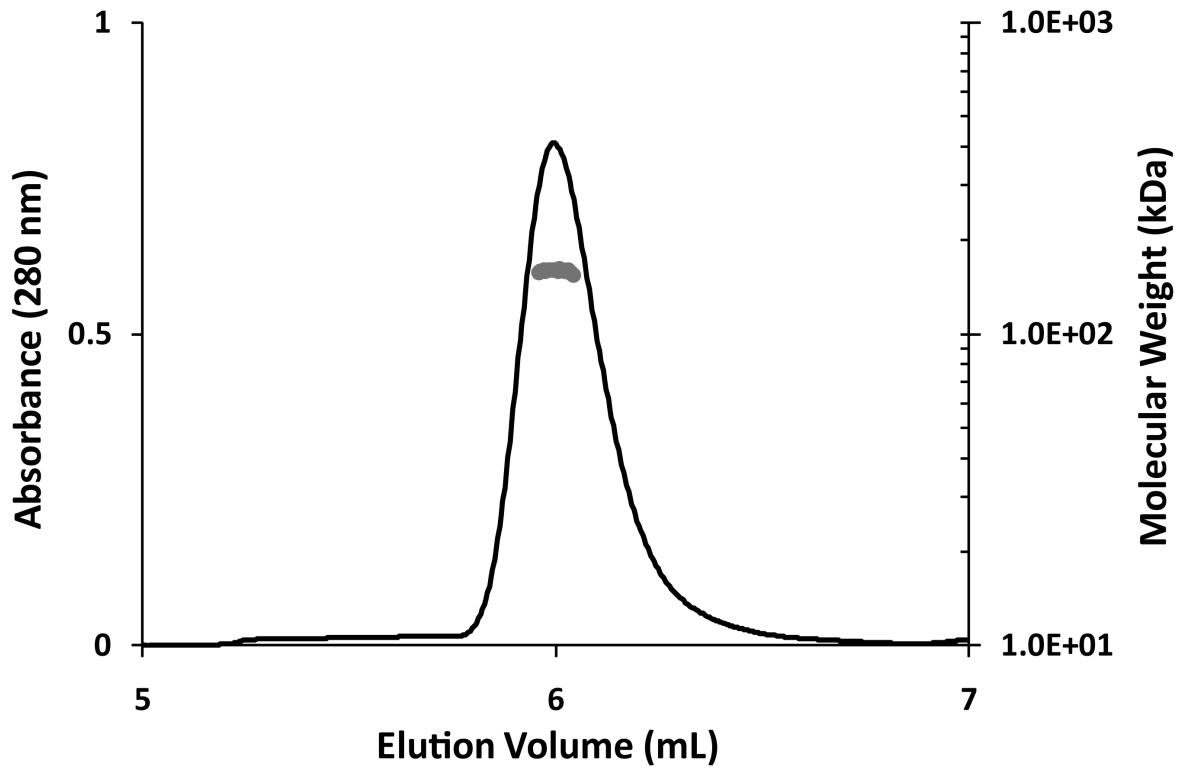
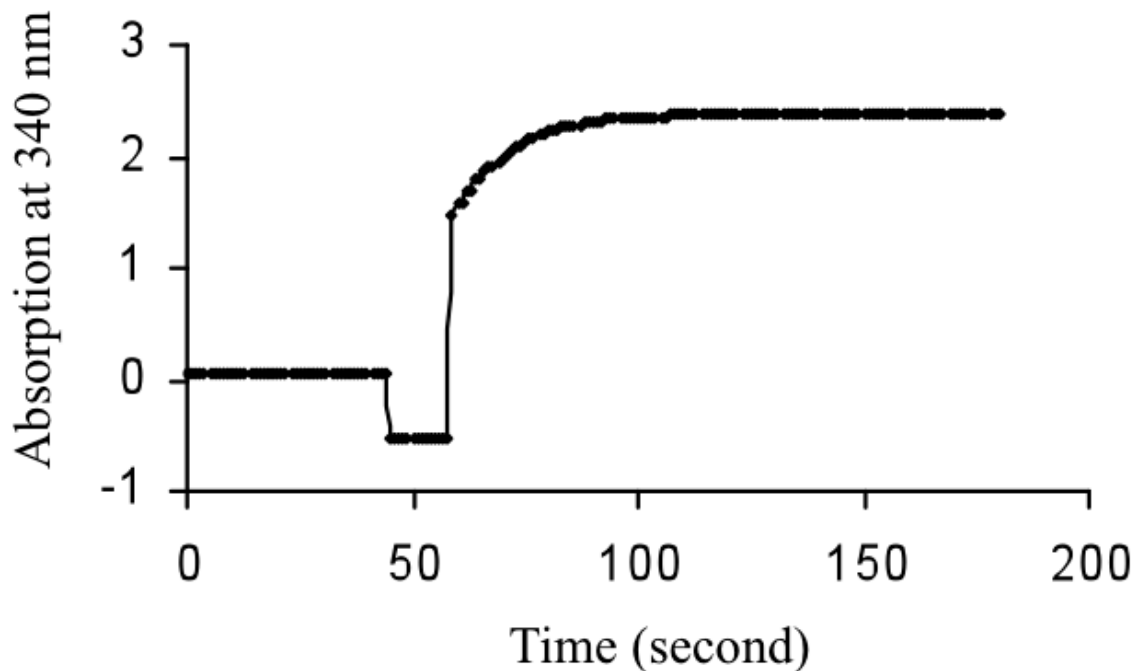


Supplemental Data 1



Multi-angle laser light-scattering elution profile of FurX. Elution profile is shown as molecular weight and absorbance *versus* elution time. The *thin* black lines represent changes in absorbance at 280 nm. The *thick red* lines indicate calculated molecular masses by the multiangle laser light-scattering pattern.

Supplemental Data2.



FurX catalyzed isopropanol-dependent reduction NAD^+ - The reaction was performed in 1 ml of the crystallization solution containing 10 mM Tris buffer (pH 8), 1 M $(NH_4)_2SO_4$, 100 mM NaCl, 2.5% isopropanol, and 400 μ M NAD^+ . The reaction was monitored for NADH production at 340 nm for 45 seconds without enzyme. Then, the sample was removed from the spectrophotometer, and 250 μ g of FurX was added in 10 μ l of volume. The sample was mixed and placed back to the spectrophotometer for continuously monitoring of NADH production. Significant reduction occurred during mixing and the reaction reached to an equilibrium within another 50 seconds of incubation. Kinetic analysis for isopropanol-dependent reduction of NAD^+ were done as reported for ethanol-dependent reduction of NAD^+ (3). The K_m values for isopropanol and NAD^+ were 14.6 ± 4.2 mM and 0.54 ± 0.10 mM, respectively. The k_{cat} was 5.1 ± 0.3 s⁻¹.

Supplemental Data3

	β1 (4-9)	β2 (18-23)	β3 (32-40)	
FurX	-----MPAMMKAAVVRAFGAPLTIDEVVPPQPGPGQVQVKIEAS			39
1LLU	-----MTLPQTMKAAVVHAYGAPLRIEEVKVPPLPGPGQVLVKIEAS			41
3MEQ	MAHHHHHHMGTLEAQTQGGPSMAKTMKAAVVRAFGKPLTIDEVPIPPQPGPGQIQVAIQAS			60
1RJW	-----MKAAVVEQFKEPLKIKEVEKPTISYGEVLVRIKAC			35
2HCY	-----SIPETQKGVIFYESHGKLEYKDI PVPKPKANELLINVKYS			40

	α1 (43-50)	β4 (67-74)	β5 (84-89)	
FurX	GVCHTDLHAAAGDWPVKPTLPFIPGHEGVGYVSAVGSVSRVKEGDRVGVWLYSACGYC			99
1LLU	GVCHTDLHAAAGDWPVKPPLPFIPGHEGVGYVAAVGSVTRVKEGDRVGIWLYTACGCC			101
3MEQ	GVCHTDLHAAAGDWPVKPNPPFIPGHEGVGFVSAVGSVGHVKEGDRVGIWLYTACGHC			120
1RJW	GVCHTDLHAAAGDWPVKPKLPLIPGHEGVGIVEEVGPGVTHLKVGDVGIWLYSACGHC			95
2HCY	GVCHTDLHAWHGDWPLPVKLLPLVGGHEGAGVVVGMGENVKGWKIGDYAGIKWLNGSCMAC			100

	α2 (100-104)	α3 (107-109)	β6 (127-130)	α4 (144-164)	
FurX	EHCLQGWETLCEKQONTGYSVNGGYGEYVVADPNYVGLLPDKVGFVEIAPILCAGVTIYK				159
1LLU	EHCLTGWETLCESEQONTGYSVNGGYAEYVADPNYVGLPKNVEFAEIAPILCAGVTIYK				161
3MEQ	RHCLGGWETLCEEQLNTGYSVNGGYAEYVADPNFVGHLPKNIDFNEIAPVLCAGVTIYK				180
1RJW	DYCLSGQETLCEHQKNAGYSVDGGYAEYCRAADYVVKIPDNLSFEAAPIFCAGVTIYK				155
2HCY	EYCELGNESNC PHADLSGYTHDGSFQQYATADAVQAAHIPQGTDLAQVAPILCAGITVYK				160

	βA (171-175)	αA (180-191)	βB (194-199)	αB (202-211)	βC (215-218)	
FurX	GLKVTDRPGQWVVISG-IGGLGHVAVQYARAMGLRVAAVDIDDAKLNLARRLGAEVAVN					218
1LLU	GLKQTNARPGQWVAISG-IGGLGHVAVQYARAMGLHVAADIDDAKLELARKLGASLTVN					220
3MEQ	GLKVTDTKPGDWVVISG-IGGLGHMAVQYARAMGLNVAAVDIDDRKLDLARRLGATVTVN					239
1RJW	ALKVGTGAKPGEWVAIYG-IGGLGHVAVQYAKAMGLNVAVDIGEKLELAKELGADLVVN					214
2HCY	ALKSANLMAGHWVAISGAAGGLGSLAVQYAKAMGYRVLIDGGEGKEELFRSIGGEVFID					220

	αC (224-232)	βD (237-240)	αD (245-254)	βE (260-263)	βF (270-273)	
FurX	AR-DTDPAAWLQKEIGG-AHGVLVTAVSPKAFSQAIGMVRGGTIALNGLPP-GDFGTPPI					275
1LLU	AR-QEDPVEAIQRDIGG-AHGVLVTAVSNSAFGQAIGMARRGGTIALVGLPP-GDFPPTPI					277
3MEQ	AKTVADPAAYIRKETDGGAQGVLTAVSPKAFEQALGMVARGGTVSLNGLPP-GDFPLSI					298
1RJW	PL-KEDAAKFMKEKVG-GVHAAVVTAVSKPAFQSAYNSTRGGACVLVGLPP-EEMPPIPI					271
2HCY	FTKEKDIVGAVLKATDGGAGHVINVSVEAAIEASTRYVRANGTTVLVGMFAGAKCCSDV					280

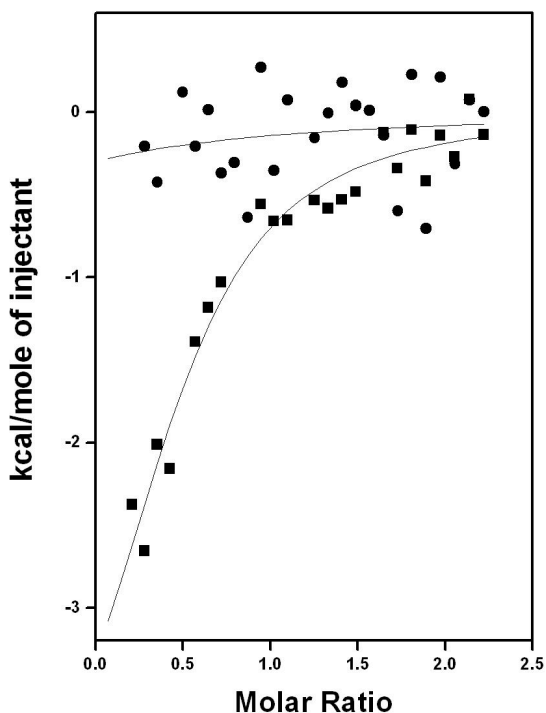
	αE (275-281)	βG (284-287)	α5 (293-305)	β7 (312-315)	α6 (320-329)	
FurX	FDVVLKGITIRGSIVGTRSDLQESLDFAAHGDVKATVSTAKLDDVNDVFGRLREGKVEGR					335
1LLU	FDVVLKGLHIAGSIVGTRADLQEQALDFAGEGLVKATIHGPKLDDINQILDQMRAGQIEGR					337
3MEQ	FNMVLNGVTVRGSIVGTRLDLQESLDFAAADGKVKATIQTGKLEDINAI FDDMRQGNIEGR					358
1RJW	FDTVLNGIKIIGSIVGTRKDLQEQALQFAAEGKVKTIIEVQPLEKINEVFDRLMLKGQINGR					331
2HCY	FNQVVKISISIVGSYVGNRADTREALDFFARGLVKSPIKVVGLSTLPEIYEKMEKQIVGR					340

	β8 (335-339)	
FurX	VVLDFSR-	342
1LLU	IVLEM---	342
3MEQ	IVMDLTQ-	365
1RJW	VVLTLEDK	339
2HCY	YVVDTSK-	347

Multiple sequence alignment between FurX and other tetrameric ADHs of high similarity.

The secondary structures of the FurX are indicated on top of the corresponding residues. The eleven residues constituting the substrate-binding pocket are shown with a yellow (one subunit) and a violet (the other subunit) color respectively. The catalytic Zn²⁺-coordinating residues, Cys42, His65 and Cys152, are indicated with a blue color and the four cysteine residues, Cys96, Cys99, Cys102 and Cys110, which coordinate the structural Zn²⁺, are indicated with a red color. His47 and Asp52, which are involved in a proton shuttling system together with Thr44, are indicated with a green color. The GxGxxG nucleotide-binding motif is depicted by red dots on top of the glycine residues. 1LLU: ADH from *Pseudomonas aeruginosa*, 3MEQ: ADH from *Brucella melitensis*, 1RJW: MDR from *Bacillus stearothermophilus*, 2HCY: ADH from *Saccharomyces cerevisiae*.

Supplemental Data4



Isothermal Titration Calorimetry (ITC) - The interactions between FurX and furfural (*filled square*), furfuryl alcohol (*filled circle*) were measured using a MicroCal VP-ITC instrument at 25°C following standard procedures. Titration buffer was 20 mM sodium phosphate buffer (pH 7.5) containing 150 mM NaCl. FurX enzyme at 0.01 mM was titrated with 0.1 mM ligands. The solutions were degassed prior to titration. Each titration experiment was performed with 29 injections of 10 μ L at 300-second equilibration intervals. Heats of dilution for an individual ligand were determined by titrating ligand into the same buffer without protein and were used to correct the protein titration. Data were fit to a single-site binding model by nonlinear least squares regression with the Origin software package. The fit of data yields the binding affinity, enthalpy change, entropy change, and binding stoichiometry for the titration.